Published in final edited form as:
J Mater Chem. 2012 October 7; 22(37): 19605–19616. doi:10.1039/C2JM34316A.

Reversible Swelling of Chitosan and Quaternary Ammonium Modified Chitosan Brush Layers: Effect of pH and Counter Anion Size and Functionality

Hyun-Su Lee[†,‡,§], **Michael Q. Yee**[§], **Yonaton Y. Eckmann**[§], **Noreen J. Hickok**[#], **David M. Eckmann**[†,‡], and **Russell J. Composto**[†,§,*]

[†]Institute of Medicine and Engineering, University of Pennsylvania, Philadelphia, Pennsylvania 19104, United States

[‡]Department of Anesthesiology and Critical Care, University of Pennsylvania, Philadelphia, Pennsylvania 19104, United States

[§]Department of Materials Science and Engineering, University of Pennsylvania, Philadelphia, Pennsylvania 19104, United States

[#]Department of Orthopaedic Surgery and Biochemistry & Molecular Biology, Thomas Jefferson University, Philadelphia, Pennsylvania 19107, United States

Abstract

This study investigates the swelling of grafted polycationic brushes as a function of pH and anion type. The brushes are chitosan (CH) and chitosans with 27% and 51% degree of substitution (DS) of quaternary ammonium salt, denoted as CH-Q_{25} and CH-Q_{50}, respectively. The water content and swelling behaviors are monitored using *in situ* quartz-crystal microbalance with dissipation (QCM-D). The pH varies from ~3.5 to 8.5, and the counter anion types include chloride, acetate, and citrate. At fixed pH, the water content and brush swelling increase as the DS increases. Whereas the CH-Q_{50} brush layer shows symmetric swelling with a minimum near pH = 4.5, the swelling of CH and CH-Q_{25} is relatively constant as pH decreases from 8.2 to 5.5, and then begins to increase near pH 4. These studies indicate that the symmetric swelling of CH-Q_{50} is likely attributed to increasing protonation of primary amines for pH values below pH 6.5 and the quaternary ammonium salts above pH 6.5. At pH 4, the swelling of the CH brush increases upon exchanging the smaller chloridewith a bulkier acetate anion, which is less effective at screening intra/inter molecular repulsion. In contrast, upon exchanging the acetate with trifunctional citrate, CH and CH-Q_{25} brushes collapse by 53 and 42%, respectively, because the citrate forms ionic cross-links. To test antibacterial properties, silicon oxide, CH and CH-Q_{50} brush layers are exposed to 10^7–10^8 cfu/ml of *S. aureus* for two days at 37 °C and exposed to stepped shear stresses in 2 min intervals. Whereas an *S. aureus* biofilm adheres strongly to silicon oxide and CH for stresses up to 12 dyne/cm^2, biofilms on CH-Q_{50} detach at a relatively low shear stress, 1.5 dyne/cm^2. Due to their high degree of swelling that can be tuned via pH, counterion size and type, chitosan and quaternary modified chitosans have potential as responsive coatings for applications including MEMS/NEMS devices and drug eluting implants.

*Correspondence should be addressed to: Russell J. Composto, Ph.D., Materials Science and Engineering, University of Pennsylvania, Laboratory for Research on the Structure of Matter, 3231 Walnut Street, Philadelphia, Pennsylvania 19104, USA. Telephone: 215 898 4451. composto@seas.upenn.edu.

Introduction

Surface chemistry provides a facile route to impart materials with complementary properties, such as stimuli-responsiveness, drug concentrating and releasing, and biocompatibility and antibacterial characteristics, attractive for biological applications. Surface coatings have been applied to medical devices such as catheters, ventilators, and stents in order to prevent complications, such as bacterial infection and blood clots caused by device insertion, without altering the device's bulk material properties. Whereas physisorbed coating provide a short term solution, synthetic and natural polymer brushes chemically grafted to the biomaterial surface[1–5] have great potential as long term, multifunction coatings.

For medical and biological applications, polymer brushes, which respond to changes in temperature, pH, and ionic strength,[6–15] have been of great interest to surface chemists. For example, neutral polymer brushes of poly(N-isoproylacrylamide) respond to changes in temperature due to a phase transition (e.g., hydrophilic/hydrophobic alterations) in water near 32 °C, which, in turn, thermally modulates surface interactions with biomolecules and cells.[7,8] Polyelectrolyte polymer brushes such as anionic poly(acrylic acid) respond to changes in ionic strength and pH by undergoing large conformational changes, and therefore can be used as a matrix for reversible immobilization of proteins and enzymes for protein separation and biosensing.[9–12] Cationic brushes of [2-(methacryloyloxy)ethyl]trimethylammonium chloride (METAC) respond to changes in ionic strength and electrolyte environment (e.g., NaCl and $MgSO_4$).[13] Recently polyelectrolyte multilayers were shown to strongly swell in a reversible manner upon exposure to stimuli such as pH and ionic strength.[14,15] These multilayers have been widely investigated because their tunable swelling properties can be used to create stimuli-responsive surfaces and interfaces for controlling drug release and modulating cell adhesion. Unfortunately, this approach is limited by the stability of the electrostatic interactions that hold the polycation and polyanion layer together.

Particularly, chitosan brush layers are an attractive coating because chitosan, which is both bio-compatible and biodegradable, has been used for medical and pharmaceutical applications such as drug delivery, tissue scaffolds, and antimicrobial coating.[16–21] Chitosan, a random-copolymer of D-glucosamine (GlcN) and N-acetyl-D-glucosamine (GlcNAc) linked by β-(1,4) glycosidic bonds, has chemical and physical properties that can be tuned by varying the mole fraction of GlcN (i.e., degree of deacetylation, DDA) or correspondingly the fraction of primary amine groups, $-NH_2$. For example, chitosan is a water-soluble cationic polyelectrolyte at low pH because the primary amines are protonated and positively charged. In contrast, at high pH (above ~6.5) chitosan is an uncharged collapsed coil that is insoluble in water. The rheological properties, solubility, and swelling of chitosan depend on pH (below ~6) and counter-anion size, because both parameters can be used to dial in the extent of intra and intermolecular electrostatic repulsion.[22–27] For drug delivery applications, ionic cross-linking of cationic chitosan with multifunctional-anions, such as sodium tripolyphosphates ($[Na^+]_5[P_3O_{10}{}^{5-}]$), has been used to fabricate stable nano-particles containing drugs and study drug delivery mechanisms.[28] For gene delivery applications, ionic complexes assembled by taking advantage of the attractive interaction between positively charged chitosan and negatively charged polyphosphate groups of DNA or RNA are of great interest.[28–31]

However, because of its limited solubility near physiological conditions (pH ~7), chitosan has not been fully utilized as a biomaterial coating. To circumvent this limitation, chitosan can be made water-soluble above pH 6.5 by modifying the molecule with quaternary ammonium salts (CH-Q).[32] For a degree of substitution of quaternary ammonium salts (DS)

equal to 0.51, we investigated the pH-dependent swelling of a CH-Q_{50} brush layer using quartz-crystal microbalance with dissipation (QCM-D) and spectroscopy ellipsometry (SE).[33] The CH-Q_{50} brush layer is chemically stable and symmetrically swells across a wide range of pH values with a minimum thickness near pH 5.0 that increases strongly at lower and higher pH. Remarkably, at pH 8, the CH-Q_{50} brush layer exhibits 900% swelling, which is much higher than typically observed for polyelectrolyte brushes.[9–12] The CH-Q_{50} brush layer is also antibacterial because of its high positive charge and strong swelling.[33]

The aim of the present study is to understand the mechanism of brush swelling for chitosan (CH) and modified chitosans (CH-Q) containing degrees of substitution (DS) of quaternary ammonium salt equal to 0.27 and 0.51. The pH-dependent swelling behavior of CH, CH-Q_{25} (DS = 0.27) and CH-Q_{50} (DS = 0.51) brush layers are monitored using *in situ* QCM-D. The pH ranges from acidic (~3.5) to slightly basic (~8.5) and counter anion types include chloride, acetate, and citrate. At each pH, the infused water content and brush swelling increases as the DS increases, namely CH < CH-Q_{25} < CH-Q_{50}. Whereas the CH-Q_{50} brush layer shows symmetric swelling behavior, the swelling of the CH and CH-Q_{25} brush layers are relatively constant between pH 8.2 and 5.5 before increasing near pH 4 (i.e., not symmetric). These swelling studies as a function of the degree of substitution of quaternary ammonium salts, indicate that symmetric swelling of CH-Q_{50} can be attributed to increasing protonation of primary amines as pH is reduced in acidic solutions and the quaternary ammonium salt moieties above pH 6.5. At fixed acidic conditions (pH 4), the swelling of the CH brush layer increases as the smaller Cl^- anion is exchanged for the bulkier $CH_3CO_2^-$, which is less effective at screening intra/inter molecular repulsion of CH. To evaluate the effect of counterion functionality, the swelling of CH and CH-Q_{25} brush layers are investigated at fixed pH 4. Upon exchanging from monofunctional acetate to the trifunctional citrate anion, the CH and CH-Q_{25} brush layers collapse by 53 and 42%, respectively, because of the ionic cross-linking mediated by the citrate anions. In preliminary tests, biofilms are found to readily detach from CH-Q_{50} brush layer at relatively low shear stress (1.5 dyne/cm^2), whereas the biofilm coverage is 90 and 60% on CH and silicon oxide, respectively, at shear stresses up to 12 dyne/cm^2.

Experimental

Materials

Chitosan Chitoclear® Cg-10 (Mw = 60 kDa and degree of deacetylation: 87%) was received from Primex ehf., Iceland. N-type, (100) oriented silicon wafers (CZ silicon: dopant, Ph: 20–30 Ω resistivity) were purchased from Silicon Quest International, USA. QCM sensor crystals, an AT-cut piezoelectric quartz crystal (14 mm in diameter and 0.3 mm thickness) coated with a 50 nm-thick layer of silicon dioxide, were purchased from Biolin Scientific, Inc. USA. 3-Glycidoxypropyl-trimethoxysilane (GPTMS, ≥ 98%), 80 wt% aqueous solution of [(2-(acryloyloxy)ethyl]trimethylammonium chloride (AETMAC), and anhydrous toluene (99.8%) were purchased from the Aldrich Chemical Co. USA. Ultrapure water (Millipore Direct-Q, 18-MΩ cm resistivity) was used for the preparation of all solutions. *Staphylococcus aureus* (*S. aureus*, ATCC™ 35556®) was obtained from PML Microbiologicals, Wilsonville, OR USA. Brain heart infusion (BHI), BBL™ trypticase™ Soy Broth (TSB), Bacto™ Agar, and Phosphate Buffered Saline tablets (PBS) were purchased from Fisher Scientific. USA.

Polymer Synthesis and Characterization

Chitosan with quaternary ammonium salts, CH-Q (see Figure 1) was prepared by Michael reaction of chitosan with acryl reagent (AETMAC) in water and characterized by using ^1H NMR experiments according to the literature.[32] ^1H NMR spectra was obtained using a

Bruker 360 MHz spectrometer in the department of chemistry at the University of Pennsylvania. The degree of substitution of the chitosan derivative, DS, was calculated by using ^{1}H NMR according to the literature.[32] For degree of deacetylation (87%, l = 0.13), 51% of monomers are functionalized with quaternary ammonium salts (DS = m = 0.51). Data for CH-Q (DS = 0.51):^{1}H NMR (360 MHz, 0.5 M DCl in D_2O, ppm) 2.06 (s, 0.39 H, NHCOCH_3), 2.91 (s, 1.01 H, -CH_2-CO_2-), 3.13 (s, NMe_3), 3.28 (s, *H-2* of GlcN), 3.31 (s, *H-2* of N-alkylated GlcN), 3.6–4.1 (m, N-CH_2- *and* -CH_2-CH_2- of N-alkyl group, *H-2* of GlcNAc, *H-3,4,5,6* of GlcN and GlcNAc), 4.61 (br, *H-1* of GlcNAc), 5.04 (br, *H-1* of N-alkylated GlcN). For degree of deacetylation (87%, l = 0.13), 27% of monomers are functionalized with quaternary ammonium salts (DS = m = 0.27). Data for CH-Q (DS = 0.27):^{1}H NMR (360 MHz, 0.5 M DCl in D_2O, ppm) 2.06 (s, 0.39 H, NHCOCH_3), 2.90 (s, 0.53 H, -CH_2-CO_2-), 3.18 (s, NMe_3), 3.22 (s, *H-2* of GlcN), 3.30 (s, *H-2* of N-alkylated GlcN), 3.5–4.1 (m, N-CH_2- *and* -CH_2- CH_2- of N-alkyl group, *H-2* of GlcNAc, *H-3,4,5,6* of GlcN and GlcNAc), 4.61 (br, *H-1* of GlcNAc), 5.08 (br, *H-1* of N-alkylated GlcN).

Surface Preparation and Characterization

Silicon wafers and SiO_2-coated QCM sensor crystals were cleaned by immersion in piranha solution (3:1 (v:v) H_2SO_4/30% H_2O_2 (Fisher Scientific)), rinsed with ultrapure water (Millipore Direct-Q, 18 MΩ-cm resistivity), dried with N_2, and exposed to UV-Ozone to produce an homogeneous hydroxylated surface and to remove impurities. Silane deposition on silicon oxide surfaces was performed by immersion of the wafers and crystals into a 10% (v/v) 3-Glycidoxypropyltrimethoxysilane (GPTMS) in anhydrous toluene at 80 °C for 12 hours under N_2 condition, respectively. The deposited samples were sonicated in toluene to remove physically absorbed GPTMS and impurities on the surface.

To immobilize CH, CH-Q_{25}, and CH-Q_{50} on epoxide-derivatized (GPTMS) silicon oxide surface, the GPTMS surface was immersed in 2 wt% aqueous solution (10 mL) of each polymers (pH ~4.5), water was evaporated slowly and the polymer films were made by direct contact with the GPTMS surface at 60 °C, overnight (~12 hrs). The surface was rinsed with the ultrapure water and acidic solution (pH~4.5) to remove physically adsorbed polymers and other impurities on the surface. For the surface characterization the dry thicknesses of CH, CH-Q_{25}, and CH-Q_{50} on the surface were measured by using a QCM-D technique, described in supporting information. Contact angles were measured by using a 1 μL sessile drop method.

In-situ Quartz Crystal Microbalance with Dissipation (QCM-D)

The QCM-D measurement is based on the resonance frequency change of a vibrating quartz crystal, a piezoelectric material, when mass is deposited on it. The deposited mass, Δm, has a relationship with the frequency change, Δf, according to the Sauerbrey equation,[33–38]

$$\Delta m = -C\frac{\Delta f_n}{n}$$

where C is the mass sensitivity constant (C = 17.7 ng·cm^{-2}·Hz^{-1} for an AT-cut, 5 MHz crystal) and n is the vibrational mode number ($n = 1, 3, 5, \cdots$). In addition, the dissipation change, ΔD_n, the loss of energy stored in a vibration cycle, indicates the physical characteristics of the deposited layer such as viscosity, elasticity, and so on. If ΔD_n is less than 2.0×10^{-6} and the plots of $\Delta f_n/n$ under several modes are superimposed, the layer is an elastic film. The physical properties (mass and thickness) of the elastic layer can be calculated using the Sauerbrey equation.[34–36] On the contrary, if ΔD_n is more than 2.0×10^{-6} and the plots of $\Delta f_n/n$ are not superimposed, the layer is viscoelastic. The physical

properties (thickness, shear modulus, and viscosity) of the viscoelastic layer can be estimated fitting between the QCM-D experimental data ($\Delta f_n/n$ ($n = 1, 3, 5, \cdots$) and ΔD_n) and a Voigt-based viscoelastic model incorporated in Q-Sense software Q-Tools.[35–37]

An E4 QCM instrument (Q-Sense Inc., Gothenburg, Sweden) was used to monitor the pH-dependent conformational changes of immobilized CH, CH-Q_{25}, and CH-Q_{50} brush layers on SiO_2-coated QCM sensor crystals. Solution pH was measured with a dual pH/conductivity meter (Dever Instru. Co. USA). The pH of the aqueous medium was adjusted to the desired value by addition of 0.1 M HCl and 0.1 M NaOH under salt-free conditions. All different pH solutions were degassed by sonication. The liquid medium was peristaltically pumped at a rate of 20 μL/min through a flow cell with the sensor crystal. The temperature of the system was controlled to 21 °C.

As a control, we first monitored $\Delta f_n/n$ ($n = 3, 5, 7$), and ΔD_n for the bare SiO_2-coated QCM sensor because changes in the solution composition can induce changes in frequency and dissipation due to variations in viscosity and elasticity. When used different pH solutions were successively introduced, $\Delta f_n/n$ was found to be constant within ± 0.5 Hz. ΔD_n was also invariant with solution composition. This shows that upon switching between the different pH solutions the observed changes in frequency and dissipation for the grafted CH, CH-Q_{25}, and CH-Q_{50} brush layers are attributed to changes in the conformation of the CH, CH-Q_{25}, and CH-Q_{50} layers as it swells or contracts.

To evaluate the effect of ionic strength, the swelling behavior of chitosan brush layers were compared at two different ionic strengths but similar pH. These two solutions (pH 4.2; Ionic strength = 80 μs/cm and pH 4.1; Ionic strength = 167 μs/cm) were adjusted by adding 1 M HCl to control pH and 5 M NaCl to vary ionic strength. Higher ionic strength solutions could not be investigated because they affect the frequency and dissipation measured by QCM-D and confound the fitting of experimental results.

In these studies, a variety of pH and counterion exposure conditions are sequentially invoked. These are summarized in Figure 2, which provides specific sequences used in the various QCM-D experiments.

Swelling of Brush Layers

To understand the pH dependent swelling behavior, the percent swelling was calculated from the dry thickness and the pH-dependent swollen thicknesses determined by *in-situ* QCM-D according to the literature.[33] The percentage swelling of the CH, CH-Q_{25}, and CH-Q_{50} layer is defined as

$$\%swelling = \frac{T_{in-situ} - T_{dry\ layer}}{T_{dry\ layer}} \times 100$$

where $T_{dry\ layer}$ is the dry thickness of the CH, CH-Q_{25}, and CH-Q_{50} layer and $T_{in\text{-}situ}$ is the each layer thickness obtained from *in-situ* method.

To understand ionic cross-linking interaction between multifunctional citrate anions and the positive charged CH and CH-Q_{25} brush layers, the percent contraction was calculated from the thickness of cationic polymer layers with mono-functional anions and the thickness of cationic polymer layers with multifunctional anions at the same pH using *in-situ* QCM-D. The percentage contraction of each layer is defined as

$$\%contraction = \frac{T_{mono-anion} - T_{multi-anion}}{T_{mono-anion}} \times 100$$

where $T_{mono\text{-}anion}$ is the thickness of the cationic polymer layer with acetic anions and $T_{multi\text{-}anion}$ is the thickness of the cationic polymer layer with citrate anions at the same pH.

Bacterial Culture and Flow Chamber Assays

Silicon oxide (as a control), CH, and CH-Q_{50} brushes on silicon oxide surfaces were used to study adhesion and detachment between bacteria/biofilm and biomaterial surfaces under physiological flowing condition. *S. aureus* (ATCC 25923) was cultured in brain heart infusion (BHI) broth, continually shaken at 175 rpm, maintained at 37 °C for 12–16 h (overnight culture) and diluted to ~1 × 10^6 cfu/ml using a 0.5 McFarland standard, a turbidity standard which is equivalent to 10^7–10^8 cfu/ml of *S. aureus* (PML Microbiologicals, Wilsonville, OR). Surfaces were immersed in the diluted bacterial solution (pH 7.3) for two days at 37 °C in 5% CO_2 to induce complete biofilm formation and surface bacterial coverage. At the end of the incubation, loosely adherent bacteria were removed, the samples were stained with SYTO-9 nucleic acid stain (Invitrogen) and then rinsed in phosphate buffered saline. For evaluation, samples were mounted onto a custom-built laminar flow chamber and imaged using an Olympus FluoView FV300 confocal microscope (4x zoom). Laminar flow with warmed PBS was initiated using a syringe pump programmed to increase incrementally the imposed shear stress from stagnation (0 dynes/cm^2) to venous (1.5, 4.3 and 6.8 dynes/cm^2) and then to arteriolar (9.4 and 11.8 dynes/cm^2) levels for two minute intervals, thus step-wise increasing the shear force and torque experienced by the adherent bacteria. Surfaces were imaged by fluorescence microscopy after each two minute perfusion epoch at each shear stress level. The partitioning of the image fluorescing/non-fluorescing area was determined using ImageJ software, from which normalized plots of bacteria areal surface coverage were derived.

Results and discussion

1. Immobilization of chitosan and quaternary ammonium modified chitosans

Recently, chitosans functionalized with quaternary ammonium salts (degree of substitution, DS = m = 0.51), CH-Q_{50}, were grafted onto GPTMS derivatized surfaces including glass, silicon with an oxide, and silicon-oxide coated QCM crystal sensor.[33] The CH-Q_{50} brushes exhibited symmetric pH-dependent swelling properties with a minimum near pH 5.[33] In order to understand the mechanism of this pH-dependent swelling, chitison with a lower quaternary ammonium salt substitution, CH-Q_{25} was prepared by a Michael reaction of chitosan, CH, (Mw = 60 kDa, degree of deacetylation = 87%, l = 0.13) with an acryl reagent (AETMAC). According to ^{1}H-NMR results of CH-Q_{25}, the monomer fractions of D-glucosamine (GlcN), N-alkylated D-glucosamine with quaternary ammonium salts (GlcN-Q), and N-acetyl-D-glucosamine (GlcNAc) are n = 0.60, m = 0.27, and l = 0.13, respectively (Table 1). These monomer fractions are in reasonable agreement with the values from the literature.[32] In the following experiments, we investigate the pH-dependent swelling of grafted CH and CH-Q_{25} brush layers to understand the role of the quaternary ammonium salt. For immobilization of CH and CH-Q_{25} on silicon oxide, the well-known epoxide-amine reaction between GPTMS-derivatized SiO_2 and primary amine of D-glucosamine in chitosan was used (Figure 1). Because CH is insoluble above ~6.5, acidic conditions (pH~4.5) were used to graft CH and CH-Q_{25} to the GPTMS surface. For comparison, CH-Q_{25} and CH-Q_{50} are soluble up to pH ~8. The dry thicknesses of the polymer brushes were determined using QCM-D, described in supporting information. This thickness is used to

determine the extent of swelling of the brush in aqueous media. For CH, CH-Q_{25}, and CH-Q_{50}, the dry masses are 2847, 1057, 456 ng/cm^2 and the water contact angles are 20, 8, and ~0, respectively (Table 1). Table 1 shows that as the GlcN-Q monomer fraction (m) increases, the dry masses and contact angles decrease. Thus, as the degree of substitution, DS, increases or GlcN monomer fraction (n) decreases, the number of primary amines available for grafting decreases and the dry thickness decreases. The decrease in contact angle (i.e., more hydrophilic) is attributed to an increase in the quaternary ammonium cations for CH, CH-Q_{25}, and CH-Q_{50}, respectively.

The radius of gyration, R_g, of the free polymer in solution can also play a role in determining the dry thickness (Table 1). As the number of quaternary ammonium cations (m) increases, the polymer grafted surface becomes more positive charged,[33] resulting in increased electrostatic repulsion between polymer chains, polymer solubility improvement, and then % swelling increase of polymer brush.[33] As a result, the radius of gyration of chitosan will increase as the degree of substitution (DS = m) increases (i.e., the number of quaternary ammonium cations increases). Figure 3 shows a cartoon representing the grafting of CH and CH-Q_{50} at the same pH (~4.5) where CH-Q_{50} is more swollen than CH (27.2 or 31.8 nm for Mw = 60 kDa, R_g (nm) = $0.064M_w^{0.55}$ or $0.075M_w^{0.55}$).[17,39,40] The large size of CH is attributed to chitosan's stiff wormlike chain characteristics as noted by its persistence length of 12 or 16 nm.[39,40] During the grafting of CH and CH-Q_{50} (Figure 1), the primary amines react with the epoxide-derivatized SiO_2 surface resulting in multiple grafting sites per molecule. Whereas end-grafted polymers can readily extend to heights much greater than R_g in good solvent,[36] polymer brushes attached by several grafting sites are not expected to swell to the same extent as end grafted polymers. The values for layer height could be 2x the radii of gyration, R_g, of the corresponding bulk chains at similar pH (Figure 3). As a result, the dry thickness of CH is greater than that of CH-Q_{50} layer and CH is expected to have a higher grafting density than the more swollen CH-Q_{50} chain (Figure 3 and Table 1).

2. *In-situ* swelling of chitosan and modified chitosan brush layers

a. Effect of pH and counteranion type on the swelling of chitosan—The water solubility and rheological behavior of chitosan in solution has been reported.[20–27] For example, chitosan behaves as a compact sphere in acetic acid containing NaCl whereas it exhibits a random coil conformation in urea solution.[23] Because pH and counteranions effect the charge density of chitosan, chain conformation and viscoelastic properties will change.[22–27] To study how charge effects swelling, chitosan (CH) was grafted to the epoxide derivatized silicon oxide and observed *in-situ* as a function of pH and counteranion types using QCM-D under a variety of conditions outlined in Figure 2(a). Figure 4(a) shows the QCM-D results for the CH brush layer on the SiO_2 coated sensor as a function of the pH of the solution. For the three modes ($n = 3, 5, 7$) compared at pH 8.02, the $\Delta f_n/n$ values superimpose, and ΔD_n exhibits its lowest value, ~ 7×10^{-6}. This result suggests that the CH brush layer exhibits elastic behavior at pH 8.02 that can be attributed to the poor solvent condition, (i.e., chitosan is insoluble in aqueous media above pH 6.5). Upon decreasing the pH from 8.02 to 3.63 (Cl^- anion) (arrow 1), $\Delta f_n/n$ ($n = 3, 5, 7$) decreases and the curves no longer superimpose; correspondingly, ΔD_n increases. This change reflects an increase of protonated amine groups within the CH brush layer leading to an increase in electrostatic repulsion and increase in water content that results in a swollen and viscous CH brush layer. Upon increasing the pH from 3.25 back to pH 8.02 (arrow 2), $\Delta f_n/n$ ($n = 3, 5, 7$) and ΔD_n return to their original values indicating that the mass of the CH layer has not changed and that CH brush layer is stable for variations in pH from 3.23 to 8.02. The increase and superposition of $\Delta f_n/n$ ($n = 3, 5, 7$) and the decrease of ΔD_n are consistent with an increase of neutral amine groups within the brush layer at high pH. As a result, the CH brush

contracts and expels water, and the original elastic, rigid layer is recovered. Upon decreasing the pH from 8.02 to 7.06 (arrow 3), $\Delta f_n/n$ ($n = 3, 5, 7$) and ΔD_n do not change. This observation suggests that the CH layer at pH 7.06 has similar properties (insolubility, elasticity) to the layer at pH 8.02. Upon deceasing the pH from 7.06 to 5.46 (arrow 4), $\Delta f_n/n$ ($n = 3, 5, 7$) and ΔD_n weakly decrease and increase, respectively. This result shows that the CH brush layer at pH 5.46 is slightly more viscous and less elastic than the layers at pH 7.06 and 8.02. When the solution pH returns to 8.02, $\Delta f_n/n$ ($n = 3, 5, 7$) and ΔD_n return to their original values. In summary, these observations show that at low pH, the CH layer swells and becomes more viscous, whereas at higher pH (pH 7.06 and 8.02), the CH layer is elastic and rigid.

In order to study the effect of counter anions on the viscoelastic and swelling properties of the CH brush layer, the brush layer was exposed to a solution at pH 3.85 containing acetate anions ($CH_3CO_2^-$) (arrow 6) for comparison with the behavior at pH 3.63 containing chloride anions (Cl^-) (arrow 1). Upon switching from pH 8.02 to pH 3.63 (Cl^-, arrow 1), $\Delta f_n/n$ ($n = 3, 5, 7$) decrease to −415, −377, and −342, respectively, and ΔD_n increases to 53.4, 48.3, and 43.1, respectively. Upon switching from pH 8.02 to pH 3.8 ($CH_3CO_2^-$, arrow 6), $\Delta f_n/n$ ($n = 3, 5, 7$) decreases to −507, −440, and −390, respectively, and ΔD_n increases to 79.1, 75.1, and 71.0, respectively. Although the CH brushes are exposed to solutions at similar pH, the decrease in frequency and increase in dissipation corresponding to the acetate anion solution (pH 3.8, $CH_3CO_2^-$, arrow 6) are bigger than those with the chloride anion solution (pH 3.63, Cl^-, arrow 1). Because they are compared at similar acidic conditions, the CH brush layers have similar concentrations of protonated amines, and therefore the main difference between environments is due to the counter anions which associate with the ammonium cation. This observation demonstrates that the bigger counter anion ($CH_3CO_2^-$) induces the layer to become more viscous and swell to a greater extent than the smaller counter anion (Cl^-). This behavior is attributed to the increased charge density in the CH brush containing the larger counter anions. After every subsequent change in pH (arrows 4, 5, 6, and 7) the brush returns to its original state at pH 8.02 indicating that swelling is reversible. In summary, these studies demonstrate that immobilized CH layer is chemically stable over a wide range of pH values and exhibit reversible swelling and contraction that can be tuned by varying the pH of the solution and counter anion type.

The thickness, shear modulus, and viscosity of the grafted layer can be calculated by fitting the Voigt based-viscoelastic model[41] with the experimental results, namely $\Delta f_n/n$ (for $n = 3, 5, 7$) and ΔD_n. The CH layer thicknesses obtained from the best fitting (Figure 4S (a)) are plotted versus time (i.e, pH) in Figure 4(b). At pH 8.20, the thickness of the chitosan layer is 53.1 ± 0.3 nm, which is similar to dry thickness of 52.7 nm (Table 1). Upon decreasing the pH from 8.20 to 3.63 (arrow 1), the layer thickness increases to 95.0 ± 0.5 nm. Upon increasing pH from 3.63 back to pH 8.20 (arrow 2), the layer thickness returns to the original value of 53.1 ± 0.3 nm. After each change in pH (arrows 4, 5, 6, and 7), the same thickness is recovered as expected for reversible behavior (arrow 1 and 2) when the solution pH returns to 8.02. Upon decreasing pH from 8.20 to 7.06 (arrow 3), the layer thickness does not change. When pH is further reduced from 7.06 to 5.46, the layer thickness increases to 55.0 ± 0.4 nm. Upon increasing pH from 5.46 to 8.20, the layer thickness returns to the original value. Thus, these results show that as pH decreases below 5.5, the thickness of CH increases, whereas above ~ pH 7 the thickness is relatively constant and is similar in value to the dry thickness. This result is consistent with the fact that chitosan is insoluble in solutions at high pH (above ~6.5).

To determine the effect of ionic strength on the swelling behavior of chitosan brush layers, the layers were exposed to solutions at similar pH (pH 4.2 and pH 4.1), but different ionic strengths (80 μs/cm and 167 μs/cm). $\Delta f_n/n$ ($n = 3, 5, 7$) and ΔD_n were monitored for the CH

brush layer upon exposure to both solutions and results are shown in Figure 5S. At the low and high ionic strengths, the swollen thicknesses were found to be very similar, 68.4 nm and 67.8 nm, respectively (Figure 5S). For the range of ionic strengths investigated, these results indicate that the swelling of the CH brush layer is mainly determined by pH.

In order to understand how swelling depends on the counter anion, CH was exposed to two different counter anions in solutions at similar pH. Whereas the CH thickness in the presence of a chloride anion at pH 3.63 is 95.0 ± 0.5 nm, the thickness is about 25% greater, 120.0 ± 0.5 nm, when coordinated with acetate anions at pH 3.85 (Figure 4(b)). This result suggests that at similar acidity, the CH swells more in the presence of the larger counter anion ($CH_3CO_2^-$) compared to the smaller counter anion (Cl^-).

b. Effect of pH on the swelling of CH-Q_{25} brush layers—To better understand how the swelling of chitosan brushes depend on quaternary ammonium salt content, *in-situ* swelling of CH-Q_{25} brushes was observed using QCM-D under a variety of conditions outlined in Figure 2(b) and compared to the behavior of CH (see prior section) and CH-Q_{50}.[33] Figure 5(a) shows the QCM-D results for the CH-Q_{25} brush layer as a function of the pH of the solution. For all three modes ($n = 3, 5, 7$), $\Delta f_n/n$ for CH-Q_{25} exposed to pH 5.46 (DI water) superimpose, and ΔD_n exhibits its lowest value, ~ 10×10^{-6}. This result suggests that the CH-Q_{25} layer behaves in an elastic manner at pH 5.46. Upon decreasing the pH from 5.46 to 3.63 in the presence of a Cl^- anion (arrow 1), $\Delta f_n/n$ ($n = 3, 5, 7$) decreases, the curves no longer superimpose, and ΔD_n increases. This observation indicates that as pH decreases the water content increases, resulting in a swollen and viscous CH-Q_{25} layer; this behavior is similar to the swelling of CH and CH-Q_{50} at low pH. Upon increasing the pH from 3.63 back to pH 5.46 (arrow 2), $\Delta f_n/n$ ($n = 3, 5, 7$) and ΔD_n return to their original values indicating that the transition is reversible. The increase and superposition of $\Delta f_n/n$ ($n = 3, 5, 7$) and the decrease of ΔD_n suggests that water is expelled from the CH-Q_{25} layer, resulting in an elastic layer at the higher pH. Upon increasing the pH further, from 5.46 to 7.06 (arrow 3), $\Delta f_n/n$ ($n = 3, 5, 7$) and ΔD_n weakly increase and decrease, respectively. Thus at pH 7.06, CH-Q_{25} layer is slightly more elastic and less viscous than at pH 5.46, which is similar to the behavior of CH shown in Figure 4. In contrast, as pH increased from 5 to 7, the CH-Q_{50} layer exhibited a decrease in frequency and increase in dissipation as a result of higher viscosity and lower elasticity.[33] When the pH returns to 5.46 (arrow 4), $\Delta f_n/n$ ($n = 3, 5, 7$) and ΔD_n return to their original values. Upon increasing the pH from 5.46 to 8.02 (arrow 5), $\Delta f_n/n$ ($n = 3, 5, 7$) and ΔD_n weakly increase and decrease, respectively, similar to the behavior at 7.06 (arrow 3). In summary, as pH decreases the CH-Q_{25} brush becomes more viscous and swells, whereas at higher pH, in the range of 7.06 to 8.02, CH-Q_{25} is more elastic and rigid with similar properties.

In order to study quaternary ammonium substitution effect on chitosan brush layer thickness (as a function of pH change), CH-Q_{25} layer thicknesses obtained from comparing the viscoelastic model[41] to experimental data ($\Delta f_n/n$ ($n = 3, 5, 7$) and ΔD_n), are plotted versus time (as a function of pH) in Figure 5(b). Upon decreasing the pH from 5.46 to 3.63 (arrow 1), the layer thickness increases to 69.0 ± 0.5 nm. Upon increasing pH from 3.63 back to pH 5.46 (arrow 2), the layer thickness returns to the original value of 43.0 ± 0.2 nm. Upon decreasing pH from 5.46 to 7.06 and 8.20 (arrows 3 and 5), the thicknesses decrease to 40.6 ± 0.3 nm and 40.4 ± 0.4 nm, respectively. At pH 7.06 and 8.20, the thicknesses of the CH-Q_{25} layer are the same and correspond to the thinnest "wet" films, which are ~2x thicker than the dry thickness of CH-Q_{25} (19.6 nm, Table 1). For the CH layer, at pH 8.20 and 7.06, the thicknesses are not significantly different and correspond to the thinnest films (53.1 ± 0.3 nm, Figure 4b) which is the same as the dry thickness (52.7 nm, Table 1). These results indicate that at pH values of 8.20 and 7.06, the CH-Q_{25} layer is swollen by water resulting in

a viscous layer, whereas the CH layer contains very little water and behaves more like a solid-like film.

c. Water content and swelling of Chitosan and Modified Chitosan brush layers—To understand the mechanism of pH dependent swelling, the water content and percent swelling of the CH, CH-Q_{25}, and CH-Q_{50} brush layers were determined from the dry and swollen QCM-D measurements at each pH and for different counter anions. Figure 6a shows the water volume fraction as a function of pH and counter anion type. At pH 7.06 and 8.20, the volume fractions of water in the CH brush are very low, only 0.01 ± 0.003 and 0.01 ± 0.002, respectively. This result is consistent with the insolubility of chitosan at pH values above ~6.5. As the pH decreases from 8.20 to 5.46, the water fraction increases to 0.06 ± 0.002. At pH 3.63 (with Cl^-), the water volume fraction is 0.43 ± 0.002, corresponding to the maximum content of water in the CH brush layer. This increase of the water solubility in the CH brush layer as the pH decreases can be attributed to the effect of an acid environment on amines. First, whereas most organic amines are insoluble in neutral water, the exposure of organic amines to aqueous HCl produces an ammonium salt, which increases the solubility in water. Thus, this increase in ammonium salt content along the CH chain elicits an increase in water infusion into the swollen layer. Second, the electrostatic repulsion between these positive charged CH chains increases the availability of free space for water infusion. Figure 6a also shows how counterion type influences the water content in the CH brush layer at fixed pH. Whereas the water volume fraction with the chloride anion (pH 3.63) is 0.43 ± 0.002, the water fraction in the CH layer increases by 30% to 0.56 ± 0.003 after exposure to the acetate anion (pH 3.85). The observed increase in water infusion into cationic polymer brushes can be attributed to the larger size of the acetate anions, which coordinate with the ammonium cations, and increase the effective electrostatic repulsion (compared to Cl^-) allowing for more space for water infusion.

The pH-dependent swelling of CH-Q_{25} brush layers was also determined and compared with the behavior of CH and CH-Q_{50}. For highly acidic conditions (pH 3 to 4, HCl), the water fractions in the CH, CH-Q_{25}, and CH-Q_{50} layers are 0.43 ± 0.002, 0.72 ± 0.003, and 0.83 ± 0.001, respectively. Thus, as the quaternary ammonium cation concentration increases (0, 0.27, and 0.51, Table 1), the volume fraction of water increases to 43%, 72%, and 83%, respectively. This behavior can be attributed to the increase in electrostatic repulsion between positively charged chains, and as a result more space for water infusion. In weak acidic solutions (pH 5 to 6), the water fractions in the CH, CH-Q_{25}, and CH-Q_{50} brush layers increases even more dramatically, to 0.06 ± 0.002, 0.54 ± 0.002 and 0.72 ± 0.002, respectively. Although the neutralized amine content along the polymer chain increases as pH increases, the CH-Q_{25} and CH-Q_{50} layers contain 54 vol% and 72vol% water, respectively. In contrast, the CH layer contains only 6 vol% water because of a net decrease in positive charge.

In neutral and basic solutions (pH ~7 and ~8.5), the collapsed CH layer contains very little infused water (~1 vol%). However, whereas the water volume fraction for CH-Q_{25} at both pH values are similar (0.51 ± 0.004, 0.51 ± 0.001, respectively). The water content of the CH-Q_{50} layer increases slightly from 80% to 90% upon increasing the pH over a similar range (i.e., 7.2 to 8.3). The different response of the CH-Q_{25} and CH-Q_{50} layers exposed to neutral and basic solutions can be attributed to their different composition. Namely, because of their different degrees of substituted quaternary ammonium cations, the brush molecules attract different concentrations of OH^- counter anions, which screen the quaternary ammonium cations, in the basic solution. Thus, as upon increasing the pH, the OH^- anions replace the Cl^- counter anions surrounding quaternary ammonium cations. For the CH-Q_{50} layer, the replacement of Cl^- with OH^- results in higher water uptake, attributed to the higher affinity of OH^- for water. In contrast, for the same change in pH from 7 to 8, the

water content in the CH-Q_{25} layer remains constant indicating that the lower concentration of the quaternary ammonium cations does not increase the OH^- counterion concentration significantly enough to increase the water content.

Figure 6b shows the percent swelling as a function of pH and counterion type. In highly acidic solutions (pH 3 to 4, HCl), CH, CH-Q_{25}, and CH-Q_{50} swell by 76%, 252%, and 476%, respectively, relative to their dry state. Although all layers are highly swollen at acidic conditions, the percent swelling linearly increases with the degree of quaternary ammonium cation substitution (DS = m). Specifically, CH-Q_{25} and CH-Q_{50} (m = 0.27 and 0.51, Table 1) swell by ~4x and ~6x the CH brush layer (m = 0), respectively. For the CH layer at the same pH, the percent swelling increases from 76% to 128% as the counterion is switched from chlorine to acetate. As pH increases (weaker acid), CH, CH-Q_{25}, and CH-Q_{50} layer swelling decreases to 6%, 107%, and 262%, respectively. In acidic solutions, the swelling of CH, CH-Q_{25}, and CH-Q_{50} increases as the pH decreases from weaker to stronger acid solutions.

In neutral and basic solutions (pH ~7 and ~8.5), CH brush layers swell by only 0.8%, the minimum value, whereas CH-Q_{25} brushes swell by 107% and 106%, respectively. As pH values of 7.17 to 8.3, CH-Q_{50} brushes swell very strongly, by 398% and 908%, respectively. Thus, under neutral and basic conditions, CH brushes do not swell, CH-Q_{25} layer with quaternary ammonium cations (DS = 0.27) shows moderate and similar swelling at both conditions, and CH-Q_{50} (DS = 0.51) shows high swelling that increases as pH increases. Whereas in acidic solution, as DS increases, the percent swelling linearly increases, in basic solution as DS increases, the percentage swelling significantly increases due to the higher water affinity of the OH^- counter anion. Also, as noted, because the quaternary ammonium cation concentration in CH-Q_{25} layer is lower, the water uptake is less and the % swelling is unaffected upon increasing the pH from 7 to 8.

In summary, the QCM-D studies of chitosan brush swelling as a function of pH show that an increase in the content of the quaternary ammonium content produces an increase in water content and, correspondingly, swelling (CH < CH-Q_{25} < CH-Q_{50}). In acidic solution, as pH decreases, the infused water content and % swelling for CH, CH-Q_{25}, and CH-Q_{50} brush layers increases because of an increase in the protonated amines (ammonium cations). In fixed acidic pH, the infused water content and % swelling of CH layers increase as the counter anion type changes from Cl^- to $CH_3CO_2^-$. This suggests that larger anions are less effective at screening the positively charged brush, resulting in greater electrostatic repulsion and swelling. In neutral and basic solutions, the CH brush thicknesses are similar to the dry values (i.e., no swelling). However, in neutral and basic solutions, the CH-Q_{25} brush thicknesses are twice the dry thickness and similar. Thus, at these conditions, the CH-Q_{25} brush shows swelling due to repulsion of the quaternary ammonium cations. For the CH-Q_{50} brush, as pH increases from neutral to basic, the percent swelling increases to its greatest value, ~900%. This observation suggests that full exchange of counter anions (Cl^- to OH^-), which coordinate with the quaternary ammonium cations, result in largest swelling behavior because OH^- has a high affinity for water. For CH-Q_{25} layer, this behavior is not observed, likely because of the lower concentration of quaternary ammonium cations and correspondingly fewer OH^- counterions.

3. Ionic cross-linking and collapse of CH and CH-Q_{25} using multifunctional counter anions

In this QCM-D study, we demonstrate that ionic crosslinking between cationic polymer layer and a multifunctional anion can be achieved using citrate anion which has been used as a citrate-based catheter lock solution to disrupt the coagulation cascade and prevent clotting.[42] Figure 7 shows the response of a CH brush layer in acidic solutions for two types of counter anions. The highly acidic solutions are prepared with acetic acid and the citric

acid at nearly the same values of pH, 4.05 and 4.08, respectively. As previously described (section 2a), the exposure of a CH brush to pH 7.06 results in a superposition of all modes (n = 3, 5, 7) and low dissipation values, consistent with a collapsed, elastic layer (5 min.). Next, a swollen cationic chitosan layer (i.e., acetate anions surround the protonated amines) is prepared by decreasing the pH from 7.06 to 4.05 (with acetate anions) (arrow 1 in Figure 7). In response, $\Delta f_n/n$ ($n = 3, 5, 7$) decreases, the curves no longer superimpose, and ΔD_n increases between 5 and 15 min exposure.

While holding pH fixed (~4), the counter anion is changed from mono-functional to multi-functional by switching from acetate to citrate anions (see Figure 2). As denoted by arrow 2 in Figure 7, $\Delta f_n/n$ ($n = 3, 5, 7$) increases, curves nearly superimpose, and ΔD_n decreases from 96.4, 77.1, and 64.7 to 25.1, 22.0, and 19.6, respectively. These changes indicate that the citrate anions have exchanged with the acetate anions and form ionic cross-links with the ammonium cations on the CH brush. The CH brush responses to the sequence of pH and anion changes are represented in Figure 8. Note that at fixed pH, the change from mono to trifunctional counteranion produces a collapsed layer due to the intra and intermolecular ionic cross-linkings. These results are consistent with the irreversibly collapse of a protein bush layer that is chemically cross-linked by oxidation.[38] Upon increasing pH from 4.08 to 7.06 (arrow 3 in Figure 7), $\Delta f_n/n$ ($n = 3, 5, 7$) does not initially respond for 5 min. and then the curves slowly approach the original value at the starting condition and superimpose after about 30 min. Similarly, ΔD_n begins to decrease about 5 min. after returning to pH 7 and then approaches its original value. This observation is consistent with an increase in the concentration of neutral amine groups within the CH layer in response to the increase in pH, which results in a release of the citrate anions and corresponding decrease in infused water content that returns the film back to its original collapsed structure (Figure 8). Overall, these experiments demonstrate that reversible swelling and collapse of CH brushes have been achieved. Furthermore, a systematic study of swelling dynamics would be of great interest to evaluate the potential for using multi-functional anions to trap and release drugs.

In addition to CH brushes, the effect of multi-functional ionic cross links on CH-Q_{25} was also performed to determine if quaternary ammonium cations perturb the previously observed behavior for CH. As described in supplement material, Figure 3S shows that CH-Q_{25} brush layers mimic the behavior of the CH brush. Namely, upon switching from acetate anions to citrate anions at nearly fixed pH (~4), the frequency and damping changes for CH-Q_{25} (arrow 2 in Figure 3S) that result from the formation of ionic cross-links are similar to the response of the CH brush shown in Figure 7. Although the thermodynamic response of CH and CH-Q_{25} to ionic crosslinking are similar, the response of cross-linked CH-Q_{25} back to its original structure (pH = 7) occurs over ~ 30min for CH and much fast, ~10, for CH-Q_{25}.

The brush layer thicknesses for CH and CH-Q_{25} are presented in Figure 8, respectively. At fixed acidic pH (~4), the thickness of the CH layer decreases from 112 nm to 53 nm upon exchanging the acetate anions for the citrate anions (arrow 2 in Figure 9(a)). For the same conditions, the thickness of CH-Q_{25} layer decreases from 81 nm to 48 nm (arrow 2 in Figure 9(b)). In acidic solution, both CH and CH-Q_{25} contract due to ionic crosslinking between the ammonium cation groups on CH and CH-Q_{25} and the citrate anions (Figure 8). The percent contraction of the CH and CH-Q_{25} brush layers are 53% and 42%, respectively. This results show that as the degrees of quaternary ammonium cation substitution of chitosan (DS = m) increase, the percent contract resulting from ionic crosslinking interaction with citrate anions decreases (CH > CH-Q_{25}). Overall observation suggests that CH layer has stronger ionic crosslinking interaction with citrate (multifunctional-anions) than CH-Q_{25} layer. These findings suggest that ionic crosslinking between positively charged chitosans and multifunctional-anions is a facile method to trap/concentrate and release active agents and

that the capacity and dynamics of the brush can be further tuned by the quaternary ammonium content in chitosan.

4. Biofilm adhesion on Chitosan and Chitosan modified brush layers

Biofilm formation on vascular catheters and endotracheal tubes is highly associated with catheter related blood stream infections[43] and ventilator associated pneumonia,[44] respectively. These pose serious risk to hospitalized patients and incur enormous costs in healthcare.[45,46] Due to either blood flow or gas motion during breathing, the biomaterial surface becomes exposed to shear stress. When bacterial adhesion strength exceeds the flow-dependent shear and torque forces resulting from blood flow or airflow, which act to remove microbes from the shear-exposed biomaterial surface, then biofilm formation and subsequent infection can ensue. Coating the surface to reduce bacterial adhesion strength is one avenue to eliminate such infections. We conducted experiments to evaluate the effects of our grafted brush layers to alter bacterial adhesion in the presence of fluid shear stress.

Fluorescence images obtained at baseline stagnation conditions (no flow, 0 dynes/cm^2) appear in Figure 10(a) and demonstrate biofilms that have formed fully on each surface, with the normalized bacterial area coverage achieving 100% levels as shown in Figure 10(b). Figure 10(a) also shows representative fluorescence images of bacteria on the three surface types at shear stress levels of 1.5 and 11.8 dynes/cm^2, respectively. The persistent fluorescence present in Figure 10(a) at the highest shear stress imposed for the silicon oxide and CH surfaces indicates a large amount of bacteria remain adherent to these surfaces, with ~ 60% areal coverage on silicon oxide and ~ 90% areal coverage on CH (Figure 10(b)). This is sharply contrasted by the results for the CH-Q_{50} surface, which are shown for duplicate experiments in Figure 10(b). The fluorescence images seen for this surface after shear exposure at 1.5 and 11.8 dynes/cm^2 appear nearly completely black (Figure 10(a)). The corresponding image intensity analysis in Figure 10(b) shows only ~ 3% residual bacterial areal coverage, or a 97% decrease in areal coverage from the zero shear condition. This is a marked improvement over the more modest 40% areal coverage reduction observed with silicon oxide and the small 10% areal coverage reduction achieved with CH coating.

While the silicon oxide and CH surfaces appear to maintain an environment favorable for biofilm formation and strong bacterial adhesion, the response of the CH-Q_{50} surface is to be wiped almost completely free of microbes even at a very low shear stress level. This result indicates the CH-Q_{50} surface has anti-adhesive properties, mostly likely related to the high swelling property of CH-Q_{50} at a biologically relevant pH (e.g., 7.3 in the culture medium) that can be exploited for anti-infection biomaterial usages. This stable CH-Q_{50} coating provides a versatile antimicrobial system that has potential applications for the biofouling, tissue engineering and medical implant communities. While previous studies have indicated the bactericidal properties of quaternary ammonium salts originate from a destabilization of the cell membrane, the molecular mechanism of the bacterial adhesion related properties of grafted polymer brushes seen here are still unverified. We anticipate that the specific role of surface structure in anti-adhesiveness will be elucidated in future work, to be performed in situ using both QCM-D and fluorescence confocal microscope.

Conclusions

In order to understand the mechanism of pH-dependent swelling, we investigated chitosan brush layers as a function of quaternary ammonium salt substitution and counterion type by grafting CH, CH-Q_{25}, and CH-Q_{50} to epoxide-derivatized silicon oxide surfaces. Using QCM-D, the dry masses, thicknesses, and grafting densities of CH, CH-Q_{25}, and CH-Q_{50} were determined under ambient conditions. *In situ* pH-dependent swelling studies of CH, CH-Q_{25}, and CH-Q_{50} were investigated by exposing these surfaces in a flow chamber to

systematic changes in pH. At fixed pH, the infused water content and swelling of the brush layers increase as the quaternary ammonium cation concentration increases, CH < CH-Q_{25} < CH-Q_{50}. In acidic solutions, the infused water content and percent swelling of CH, CH-Q_{25}, and CH-Q_{50} brush layers increase as pH decreases. Protonated amines (ammonium cations) of each polymer layers affect swelling behavior of the chitosan layers. At the same acidic condition, the percent swelling of the CH brush layer increases as the counter anion size increases (i.e., Cl^- to $CH_3CO_2^-$). We attribute this increase in swelling and water content to a decrease in the screening of the charged grafted CH molecules in the presence of the bulkier counter anion. For neutral and basic solutions, the thicknesses of the CH brush layers are similar to the dry thicknesses, consistent with the insolubility of chitosan at pH values above ~6.5. The swelling of the CH-Q_{25} brush layer is similar at neutral and basic conditions because the quaternary ammonium cation dictates electrostatic repulsion. As the pH increases from neutral to basic, the CH-Q_{50} brush layer exhibits a strong swelling transition and reaches 900% near a pH of 8. We attribute this behavior to a complete exchange of counter anions from Cl^- to OH^-, which surround the quaternary ammonium cations and increase the influx of water due to the strong affinity of the OH^- counter anion for water. For the CH-Q_{25} brush layer, this strong swelling behavior may be absent because of the quaternary ammonium cation content is below a critical value.

We also demonstrate that the collapse and expansion of chitosan and CH-Q_{25} brush layers can be driven by exposing these layers to citrate anions which produce ionic cross-links within the brush. At pH 4, as DS increases, the percent contraction due to ionic cross-linking mediated by citrate anions decreases (CH > CH-Q_{25}). Upon increasing the pH from 4 to 7, the citrate anions in the CH brush layer are released over ~30 min. with the brush returning to its original collapsed state. The release of the citrate anions from the CH-Q_{25} layer is slower and occurs over ~10 min. before the original structure is recovered at pH 7. For gene delivery systems, ionic cross-linking between positively charged chitosans and multifunctional-anions (such as negatively charged DNA and RNA) can be tuned by varying the quaternary ammonium cation content in the chitosan. The adhesion of biofilms was studied using flow dynamics. The CH-Q_{50} brush layer showed the weakest bacterial adhesion compared to silicon oxide surface and CH brush layer. The large swelling behavior of the CH-Q_{50} brush layer may be responsible for the low adhesion of the biofilm. To better understand the antimicrobial properties of CH, CH-Q_{25}, and CH-Q_{50} brush layers bacterial adhesion studies are underway using a combination of fluorescent imaging, a parallel plate flow chamber adhesion apparatus and QCM-D.

Supplementary Material

Refer to Web version on PubMed Central for supplementary material.

Acknowledgments

This work was supported by the National Institutes of Health (NIH R01 HL60230, DME). R.J.C. also thanks Colgate-Palmolive, Johnson and Johnson, the Nanotechnology Institute, and the NSF/NBIC program for partial support.

References

1. Senaratne W, Andruzzi L, Ober CK. Biomacromolecules. 2005; 6:2427. [PubMed: 16153077]
2. Halperin A, Tirrell M, Lodge TP. Adv Polym Sci. 1992; 100:31.
3. Milner ST. Science. 1991; 251:905. [PubMed: 17847384]
4. Zhao B, Brittain WJ. Prog Polym Sci. 2000; 25:677.
5. Zdyrko B, Luzinov I. Macromol Rapid Commun. 2011; 32:859. [PubMed: 21509848]

6. Stuart MAC, Huck WTS, Genzer J, Muller M, Ober C, Stamm M, Sukhorukov GB, Szleifer I, Tsukruk VV, Urban M, Winnik F, Zauscher S, Luzinov I, Minko S. Nature Materials. 2010; 9:101.
7. Abu-Lail NI, Kaholek M, LaMattina B, Clark RL, Zauscher S. Sensor Actuat B-Chem. 2006; 114:371.
8. Mizutani A, Kikuchi A, Yamato M, Kanazawa H, Okano T. Biomaterials. 2008; 29:2073. [PubMed: 18261791]
9. Ayres N, Boyes SG, Brittain WJ. Langmuir. 2007; 23:182. [PubMed: 17190502]
10. Wu T, Gong P, Szleifer I, Vlcek P, Subr V, Genzer J. Macromolecules. 2007; 40:8756.
11. Jhon YK, Bhat RR, Jeong C, Rojas OJ, Szleifer I, Genzer J. Macromol Rapid Commun. 2006; 27:697.
12. Zhou J, Lu X, Hu J, Li J. Chem Eur J. 2007; 13:2847. [PubMed: 17183600]
13. Moya S, Azzaroni O, Farhan T, Osborne VL, Huck WTS. Angew Chem Int Ed. 2005; 44:4578.
14. Hiller J, Rubner MF. Macromolecules. 2003; 36:4078.
15. Itano K, Choi J, Rubner MF. Macromolecules. 2005; 38:3450.
16. Ravi Kumar MNV, Muzzarelli RAA, Muzzarelli C, Sashiwa H, Domb AJ. Chem Rev. 2004; 104:6017. [PubMed: 15584695]
17. Rinaudo M. Prog Polym Sci. 2006; 31:603.
18. Kim I, Seo S, Moon H, Yoo M, Park I, Kim B, Cho C. Biotechnology Advances. 2008; 26:1. [PubMed: 17884325]
19. Rabea EI, Badawy ME–T, Stevens CV, Smagghe G, Steurbaut W. Biomacromolecules. 2003; 4:1457. [PubMed: 14606868]
20. Yi H, Wu L, Bentley WE, Ghodssi R, Rubloff GW, Culver JN, Payne GF. Biomacromolecules. 2005; 6:2881. [PubMed: 16283704]
21. Payne GF, Raghavan SR. Soft Matter. 2007; 3:521.
22. Hamdine M, Heuzey M, Begin A. Int J Biol Macromol. 2005; 37:134. [PubMed: 16257048]
23. Chen RH, Lin WC, Lin JH. Acta Polym. 1994; 45:41.
24. Sakiyama T, Chu C, Fujii T, Yano T. J Appl Polym Sci. 1993; 50:2021.
25. Pack JW, Choi K, Pack KK. Bull Kor Chem Soc. 1983; 4:68.
26. Rinaudo M, Milas M, Dung PL. Int J Biol Macromol. 1993; 15:281. [PubMed: 8251442]
27. Berth G, Dautzenberg H. Carbohydr Polym. 2002; 47:39.
28. Csaba N, Koping-Hoggard M, Alonso MJ. Int J Pharm. 2009; 382:205. [PubMed: 19660537]
29. Morille M, Passirani C, Vonarbourg A, Clavreul A, Benoit JP. Biomaterials. 2008; 29:3477. [PubMed: 18499247]
30. Dang JM, Leong KW. Adv Drug Deliv Rev. 2006; 58:487. [PubMed: 16762443]
31. Liu X, Howard KA, Dong M, Andersen MO, Rahbek UL, Johnsen MG, Hansen OC, Besenbacher F, Kjems J. Biomaterials. 2007; 28:1280. [PubMed: 17126901]
32. Sashiwa H, Yamamori N, Ichinose Y, Sunamoto J, Aiba S. Biomacromolecules. 2003; 4:1250. [PubMed: 12959591]
33. Lee H, Eckmann DM, Lee D, Hickok NJ, Composto RJ. Langmuir. 2011; 27:12458. [PubMed: 21894981]
34. Sauerbrey G. Z Phys. 1959; 155:206.
35. Vogt BD, Lin EK, Wu W, White CC. J Phys Chem B. 2004; 108:12685.
36. Lee H, Penn LS. Macromolecules. 2008; 41:8124.
37. Lee H, Penn LS. Langmuir. 2009; 25:7983. [PubMed: 19388629]
38. Hook F, Kasemo B, Nylander T, Fant C, Sott K, Elwing H. Anal Chem. 2001; 73:5796. [PubMed: 11791547]
39. Anthonsen MW, Varum KM, Smidstrod O. Carbohydrate Polymers. 1993; 22:193.
40. Cho J, Heuzey M, Begin A, Carreau PJ. J Food Eng. 2006; 74:500.
41. Aklonis, JJ.; Knight, WJ. Introduction to Polymer Viscoelasticity. 2. Vol. Chapter 7. John Wiley & Sons; New York: 1983.

42. Shah CB, Mittelman MW, Costerton JW, Parenteau S, Pelak M, Arsenault R, Mermel LA. Antibicrob Agents Ch. 2002; 46:1674.

43. O'Grady NP, Alexander M, Burns LA, Dellinger P, Garland J, Heard SO, Lipsett PA, Masur H, Mermel LA, Pearson ML, Raad II, Randolph A, Rupp ME, Saint S. Am J Infect Control. 2011; 39:S1. [PubMed: 21511081]

44. Pneumatikos IAM, Dragoumanis CKM, Bouros DEM. Anesthesiology. 2009; 110:673. [PubMed: 19212256]

45. Maki DG, Kluger DM, Crnich CJ. Mayo Clin Proc. 2006; 81:1159. [PubMed: 16970212]

46. Eagye KJM, Nicolau DPP, Kuti JLP. Sem Resp Crit Care M. 2009; 30:116.

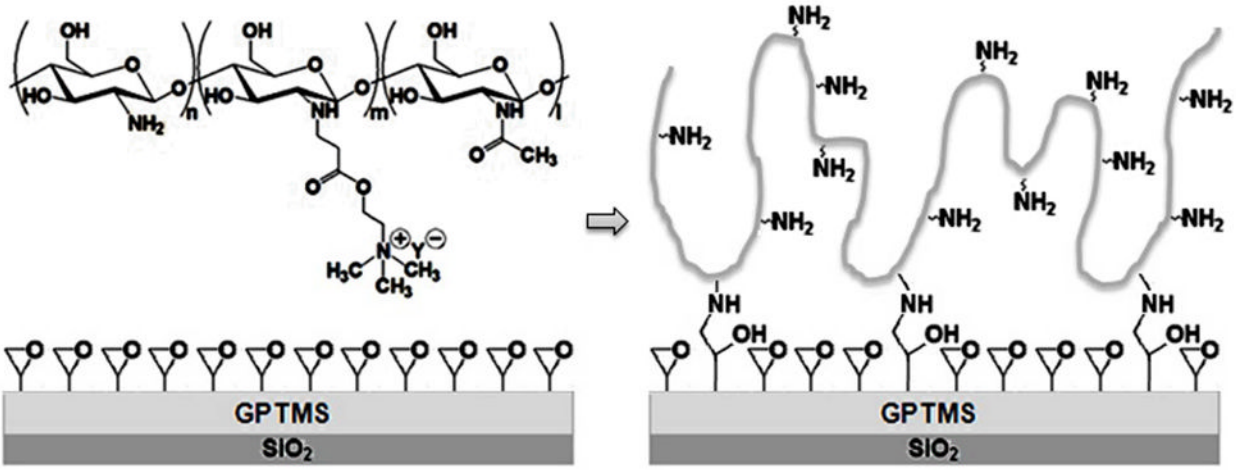

Figure 1.

(Left) The chemical structure of chitosan (CH, m=0, degree of deactylation: 87%) and chitosan modified with quaternary ammonium salts (CH-Q_{25}, m=0.27; CH-Q_{50}, m=0.51). (Right) Chitosan is "grafted to" epoxide-derivatized silicon oxide via the primary amine groups.

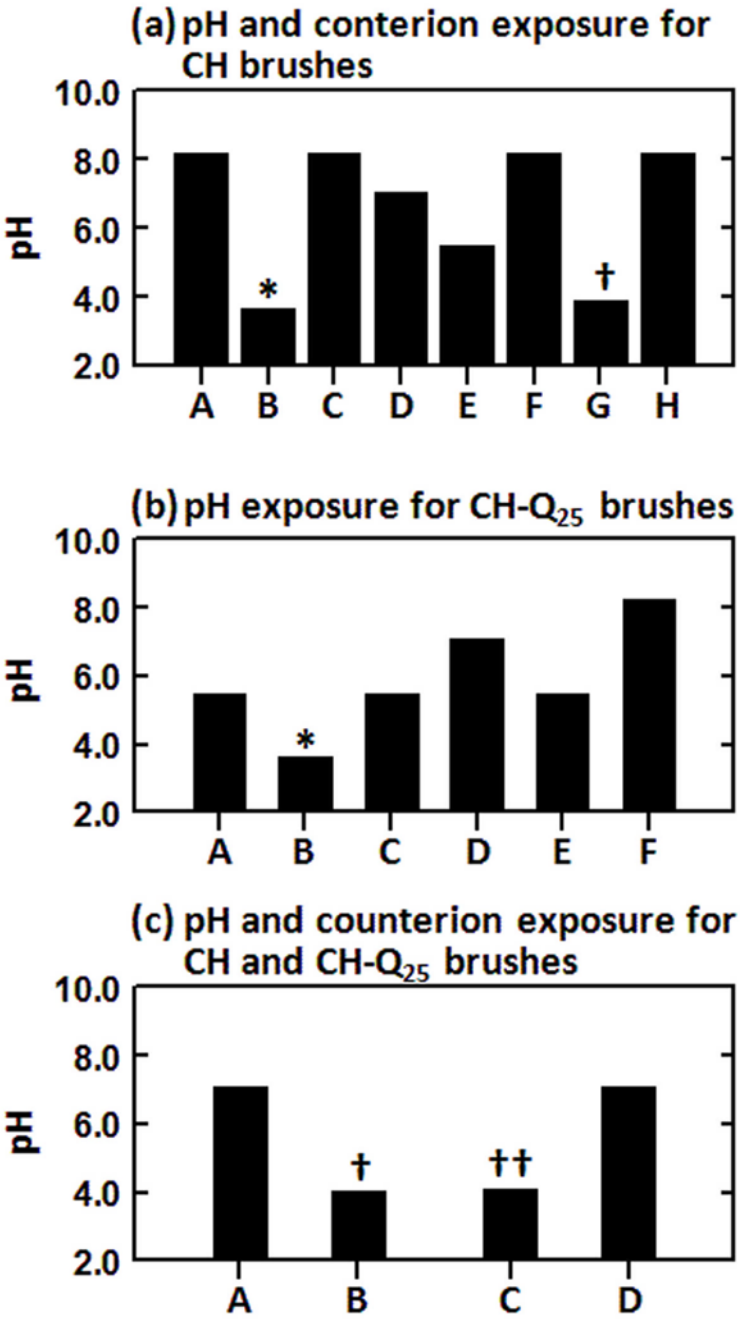

Figure 2.

A variety of pH and counterion exposure conditions, sequentially invoked, and specific sequences used in QCM-D experiments ((a), (b), and (c)). Counteranions in acidic solutions: *chloride anions, †acetate anions, ††citrate anions.

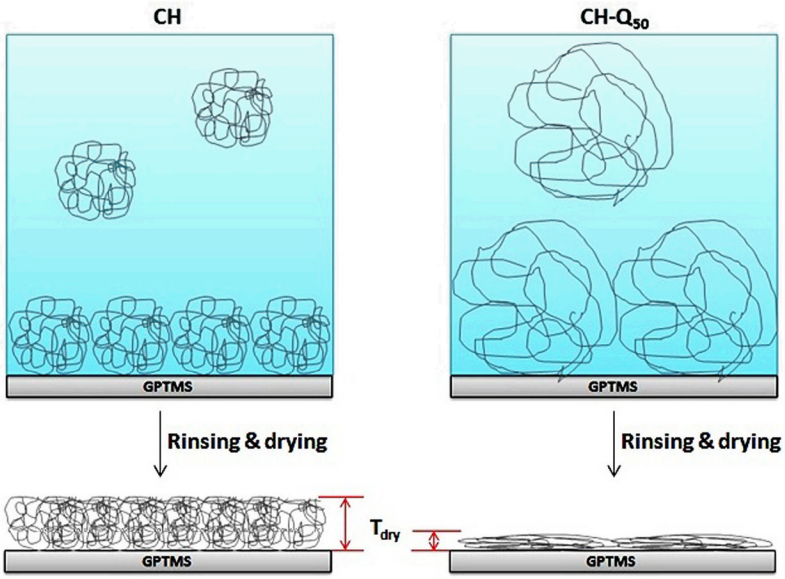

Figure 3.

Whereas chitosan (left) has a smaller radius of gyration, Rg, than CH-Q_{50} (right), when deposited at pH ~4.5, the more collapsed state leads a more dense layer of polymer. However, the more expanded CH-Q_{50} blocks a larger area per molecule via repulsive interactions resulting in a thinner polymer layer when dried.

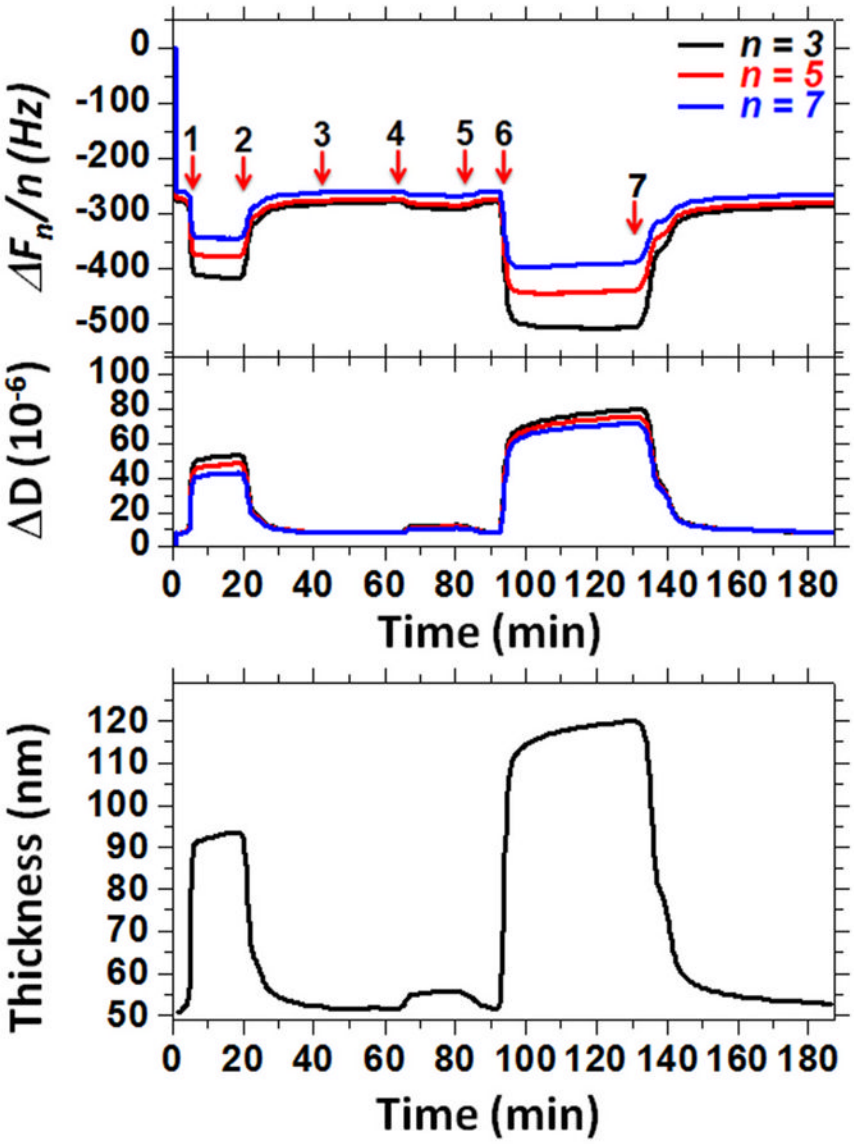

Figure 4.

(a) Traces of $\Delta f_n/n$ ($n = 3, 5, 7$) and ΔD_n of CH brush versus time as a function of sequential changes of solution pH and counteranion type such as chloride and acetate. Arrows 1, 2, 3, 4, 5, 6, and 7 represent pH changes from 8.20 to 3.63 (Cl^-), 3.63(Cl^-) to 8.20, 8.20 to 7.06, 7.06 to 5.46 (DI water), 5.46 (DI water) to 8.20, 8.20 to 3.85 (with $CH_3CO_2^-$), and 3.85 (with $CH_3CO_2^-$) to 8.20, respectively. (b) Thickness versus time determined from the best fit (Figure 4S (a)) of the QCM-D data with the viscoelastic model.[41]

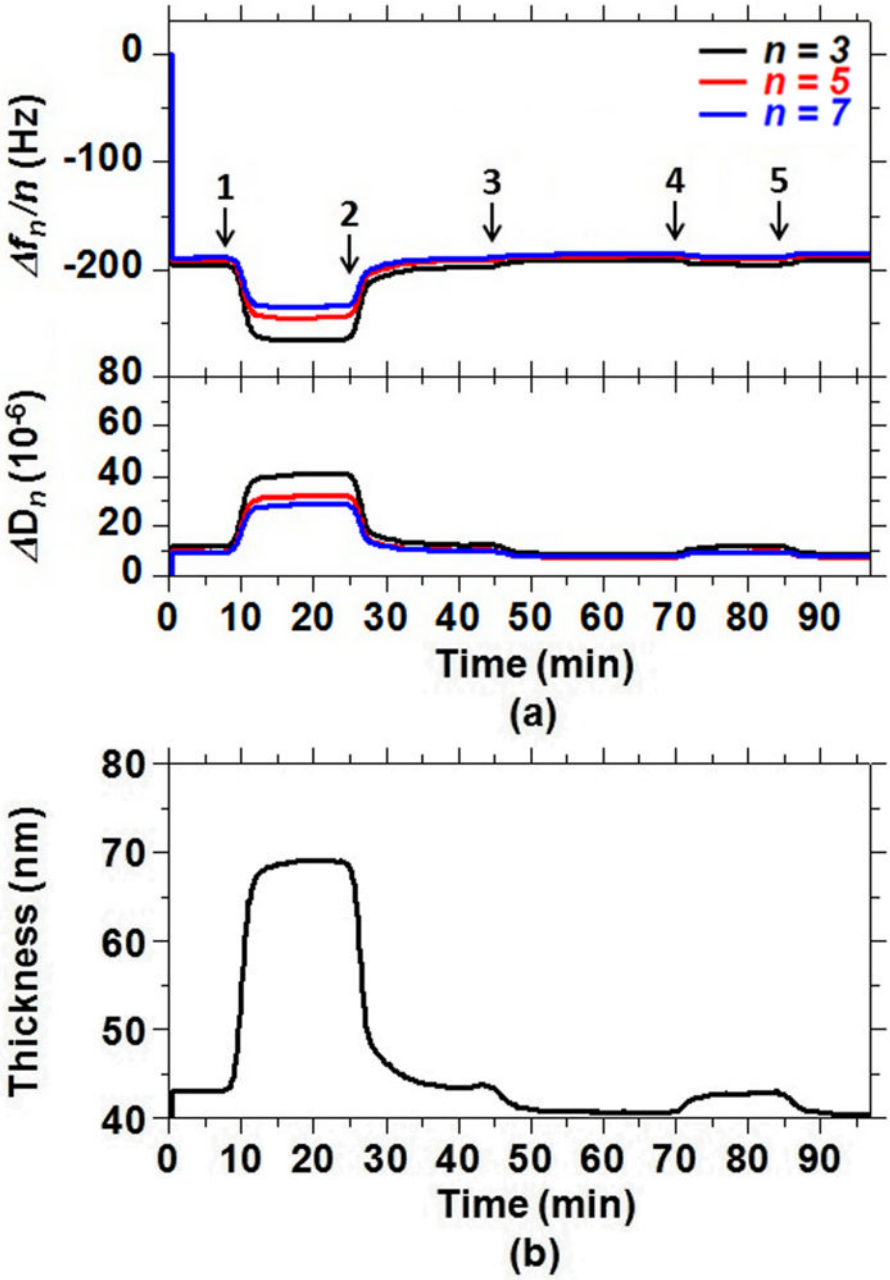

Figure 5.

(a) Traces of $\Delta f_n/n$ ($n = 3, 5, 7$) and ΔD_n versus time for grafted CH-Q_{25} as a function of sequential changes of the solution pH. Arrows 1, 2, 3, 4, and 5 represent the change from pH 5.46 to pH 3.63 (Cl^- anion), pH 3.63(Cl^- anion) to pH 5.46, pH 5.46 to 7.06, pH 7.06 to 5.46 (DI water), and pH 5.46 to 8.20, respectively. (b) Thickness versus time determined from the best fit (Figure 4S (b)) of the QCM-D data with the viscoelastic model.[41]

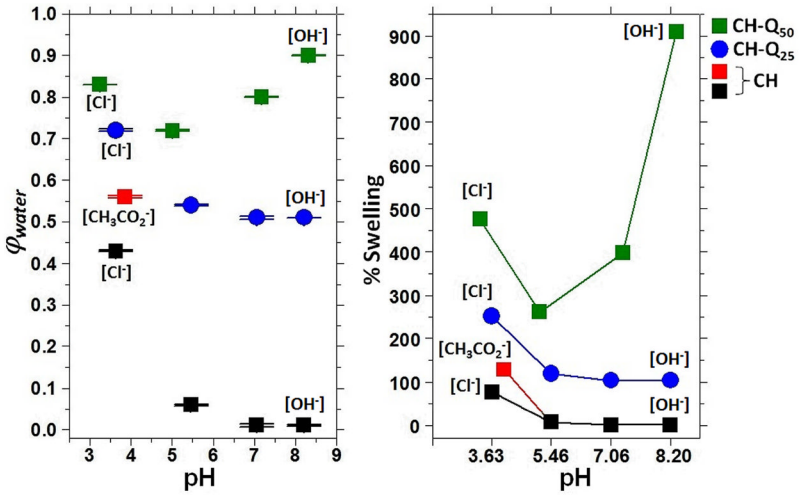

Figure 6.

(a) *In situ* QCM-D measurements of the infused water fractions in CH, CH-Q_{25}, and CH-Q_{50} layers as a function of solution pH. (b) Percent swelling of CH, CH-Q_{25}, and CH-Q_{50} layers at each pH. [$CH_3CO_2^-$] represents an acidic solution (pH 3.85) prepared with acetic acid. [Cl^-] represents acidic solutions (pH 3.25 and 3.63) prepared with hydrogen chloride. [OH^-] represents basic solutions (pH 8.2 and 8.3) prepared with sodium hydroxide

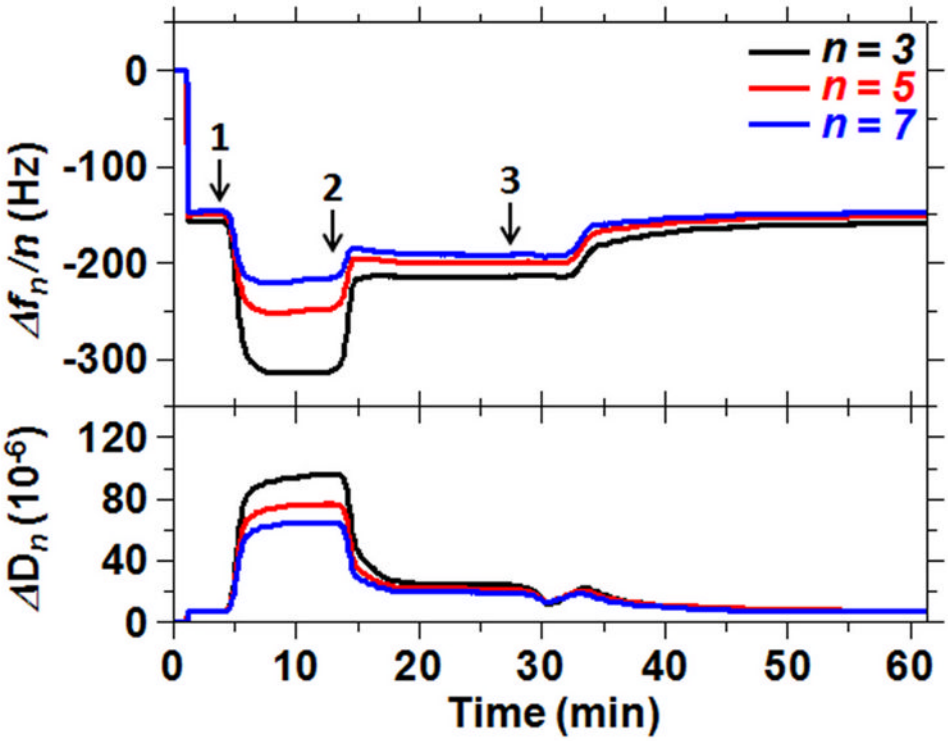

Figure 7.

Traces of $\Delta f_n/n$ ($n = 3, 5, 7$) and ΔD_n of CH layer vs time as a function of sequential changes in solution pH. Arrows 1, 2, and 3 represent the change from pH 7.06 to pH 4.05 (with acetate anions), pH 4.05 to pH 4.08 (with citrate anions), pH 4.08 to pH 7.06, respectively.

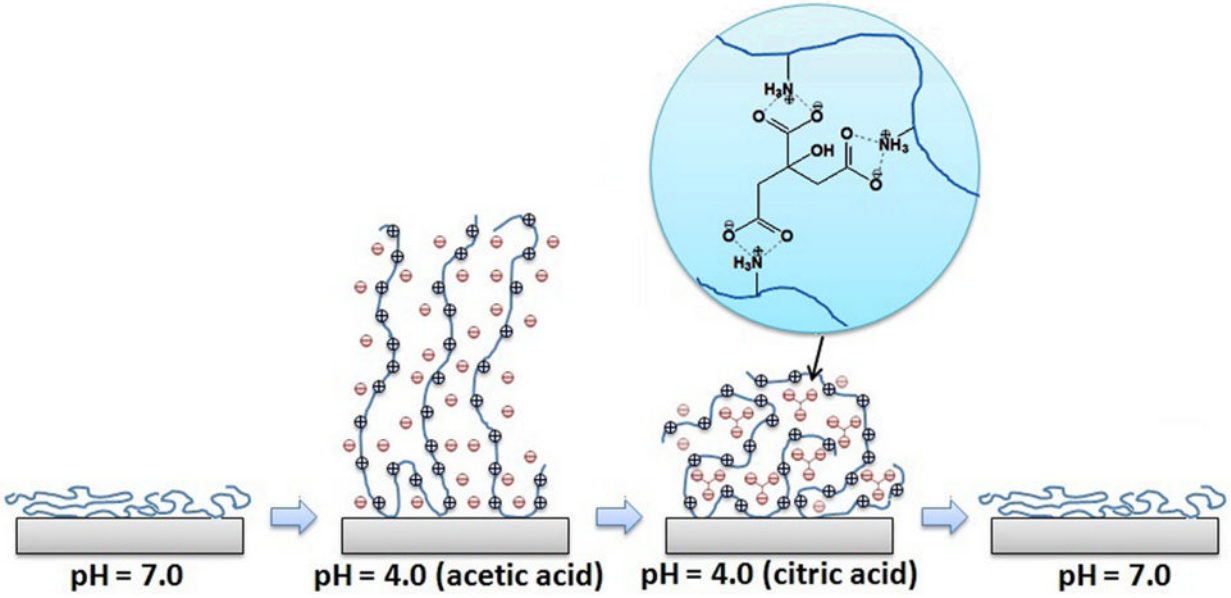

Figure 8.

Schematic showing the structure of the chitosan brush layer as a function of pH and counter anion type. Upon decreasing pH from neutral (7.0) to acidic (pH =4) by adding acetate anions, the brush swells due to electrostatic repulsion. At fixed pH = 4, an exchange of the mono-functional acetate anion with the multifunctional citrate anion leads to a shrinking of the chitosan brush layer because the citrate cross-links the brush. Upon changing to neutral conditions, the brush returns to its original collapsed state demonstrating the swelling behavior of the brush is reversible.

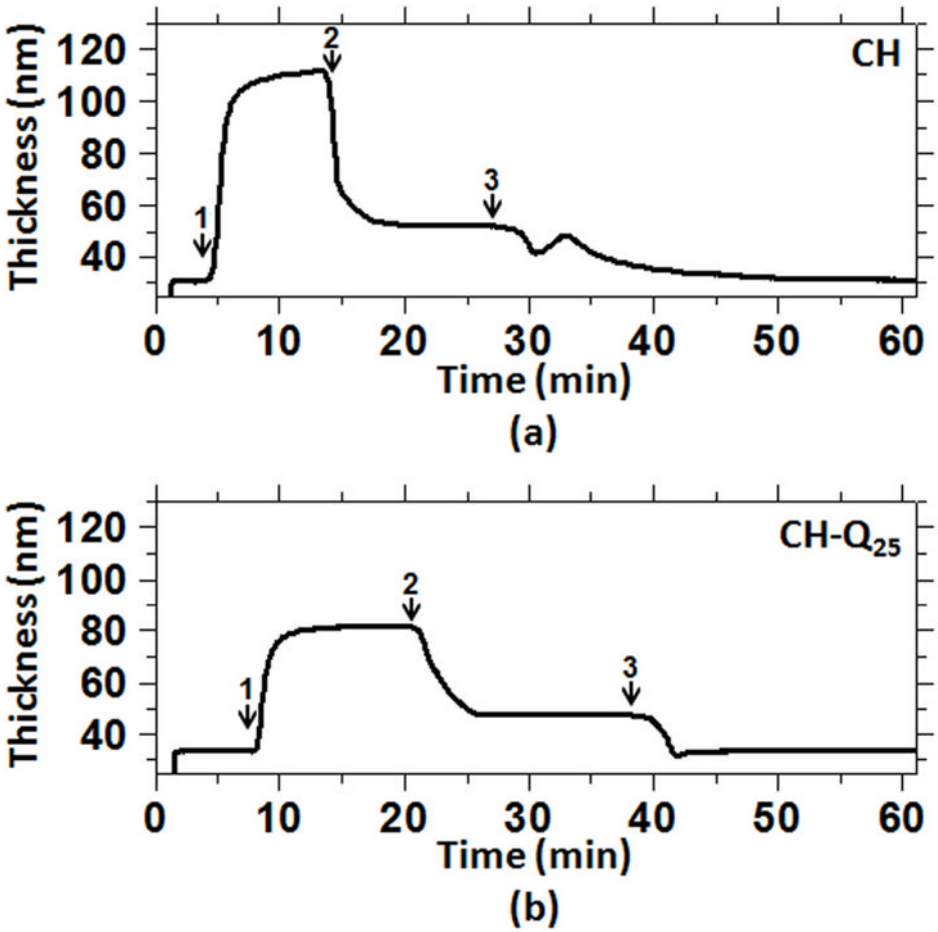

Figure 9.

The thickness of CH (a) and CH-Q_{25} (b) brush layers as a function of sequential changes in solution pH. Arrows 1, 2, and 3 represent the change from pH 7.06 to pH 4.05 (acetate anions), pH 4.05 to pH 4.08 (citrate anions), and pH 4.08 to pH 7.06, respectively. The thicknesses of CH and CH-Q_{25} were determined from the best fit (Figure 4S (c) and (d)) of each experimental data with the viscoelastic model.[41]

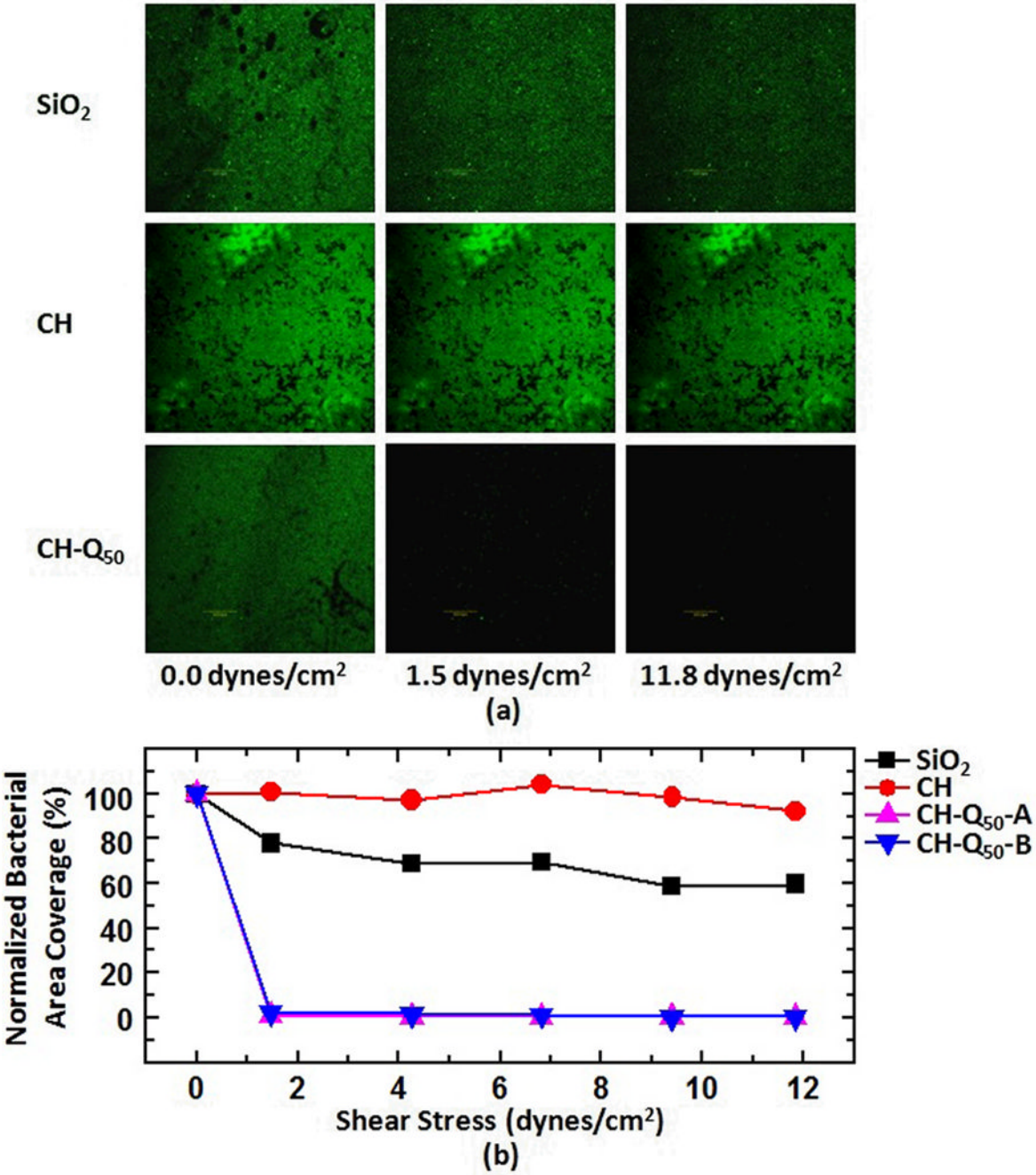

Figure 10.

(a) Confocal fluorescence microscopy images of bacteria on SiO_2, CH and CH-Q_{50} surfaces at shear stress levels of 0, 1.5 and 11.8 dynes/cm^2. (b) Normalized bacterial area coverage (%) for SiO_2, CH and CH-Q_{50} surfaces as a function of shear stress level. CH-Q_{50}-A and CH-Q_{50}-B represent duplicate experiments.

Table 1

Mass, grafting density, dry thickness, and contact angle for polymer brushes

Grafted polymer	Monomer fractions of polymer			Mass (ng/cm^2)[a]	Grafting density (chains/nm^2)[b]	Thickness (nm)[c]	Contact angle (°, DI water)
	n	m	l				
CH	0.87	0	0.13	2847	0.29	52.7	20. ± 7
CH-Q_{25}	0.60	0.27	0.13	1057	0.11	19.6	8. ± 3
CH-Q_{50}	0.36	0.51	0.13	456	0.05	8.4	~0

[a,b,c] Dry masses, grafting densities, and dry thicknesses were determined using the Sauerbrey equation, chitosan molecular weight, and density (cg10: Mw = 60 kDa, density = 0.54 g/cm^3). Details are given in supporting information.